TÜBİTAK

Turkish Journal of Earth Sciences
http://journals.tubitak.gov.tr/earth

Research Article

Turkish J Earth
(2021) 45: 639-652

doi: 10.3906/yer-2102-13

A Holocene paleomagnetic record from Küçükçekmece Lagoon, NW Turkey

Özlem MAKAROĞLU*
İstanbul University-Cerrahpaşa, Engineering Faculty, Geophysics Department, İstanbul, Turkey

Received: 02.03.2021 **Accepted/Published Online:** 22.07.2021 **Final Version:** 28.09.2021

Abstract: Lake sediments are very useful for providing high-resolution records of geomagnetic field variations, especially for the Holocene period. We present high-resolution paleomagnetic records from three cores (KCL12P1, P2, and P3) recovered from Küçükçekmece Lagoon, located at the northern shoreline of the Sea of Marmara, Turkey. The cores were subjected to a comprehensive paleomagnetic and rock magnetic investigation using oriented samples. According to the age-depth model, based on radiocarbon dating and X-ray fluorescence-derived Ca/Ti element ratios, tuned to available oxygen isotope records based on an absolute calendar-year time-scale, we obtained a new paleomagnetic record for the last 3800 years. Low paleointensities were found during 1500–2000 BP. Stacked paleomagnetic directions from Küçükçekmece Lagoon were correlated to regional geomagnetic field models. This correlation proved that the paleomagnetic records (paleointensity, inclination) obtained from the Küçükçekmece Lagoon sediments considerably agree with the data from the surrounding region over the past 3800 years.

Key words: Paleomagnetism, paleosecular variation, Holocene, Küçükçekmece Lagoon, İstanbul, NW Turkey

1. Introduction

The investigation of paleomagnetic records from lake sediments, continuously deposited over geological times, is essential to understand the dynamic of the Earth magnetic field and the construction of age models of lacustrine sediments. Such age models can be created by comparing newly obtained paleomagnetic records to published paleomagnetic secular variation (PSV) reference data (Snowball et al., 2007; Haltia-Hovi et al., 2010; Ledu et al., 2010; Mensing et al., 2015; Lapointe et al., 2019) and geomagnetic field models (Brown et al., 2015; Nilsson et al., 2014) which summarize paleomagnetic data on a larger scale. Short-term and small amplitude departures in direction (declination and inclination) and intensity of the geomagnetic field are termed PSV. A reliable correlation of these records is solely possible on a regional scale of a few thousand kilometers. Thus, increasing the number of paleomagnetic records on a regional scale is quite crucial. There are many Holocene paleomagnetic records from lakes located in the different regions of the Earth such as America (Gogorza et al., 2000), Europe (Mothersill, 1996; Saarien, 1998; Brandt et al., 1999; Gogorza et al., 2000; Kotilainen et al., 2000; Nourgaliev et al., 2000; Snowball and Sandgren, 2002; Haltia-Hovi et al., 2010), New Zealand (Anker et al., 2001) and Antarctica (Sagnotti et al., 2001), whereas there are just a few results from the Middle and Near East (Thompson et al. 1985; Frank et al., 2002, 2007; Shaar et al., 2018). In Turkey, there is a scarcity of PSV records over the Holocene. The studies of high-resolution paleomagnetic record over the last 9000 years and 350 ka in Turkey were performed by Makaroğlu (2011) and Vigliotti et al. (2014), respectively, in Lake Van located in eastern Anatolia. The studies showed that the paleomagnetic records of the lake are not of high quality due to low NRM intensities. The work of Drab et al. (2015) showed that the magnetic records obtained from the Marmara Sea, located in NW Turkey, are affected by intense early diagenesis for the last 2000 years. Another comprehensive paleomagnetic study was performed on sediments from the Sea of Marmara covering the last 70 ka. The well-dated and high-resolution paleomagnetic record also shows a reliable paleosecular variation even with some excursions recorded (Makaroğlu et al., 2020). Archaeomagnetic studies also revealed reliable PSV records and it was possible to correlate these records with the paleomagnetic records from lakes. A well-dated and high-resolution archaeomagnetic data are available from Bulgaria (Kovacheva, 1980), which is close to the study area. There are just a few paleointensity studies from archeologic artifacts (Korfmann and Becher, 1987; Sanver and Ponat, 1981; Ponat, 1995; Sarıbudak and Tarling, 1993; Sayın and Orbay, 2003; Ertepınar et al., 2012, 2016, 2020) and volcanic areas (Kaya, 2020) in Turkey. However, these are not useful features for correlation since they don't represent continuous records even they are of good quality and provide absolute paleointensity data. Several global geomagnetic field models have also been developed and renewed by archaeological and lacustrine data. CALS3k.4 (Korte and Constable, 2011), ARCH3K.1 (Korte et al., 2009), and CALS10k.1 (Korte et al., 2011) for the past 3 and 10 kyr, respectively, which are being used frequently for correlation purposes. Another reference data set are the regional PSV master curves commonly used, like geomagnetic field models. These curves are created for certain regions such as Fennoscandia (Snowball et al., 2007), United Kingdom (Thompson and Turner, 1979), North Sweden (Snowball

* Correspondence: ozlemm@istanbul.edu.tr

and Sandgren, 2002), Italy (Vigliotti, 2006). These data compilations are also very useful for correlations and the creation of age models by tuning new data to these master records, but still they should be used just over distances on the order of about 2000 km.

Here, this paper presents the results from a comprehensive paleomagnetic investigation of the sediments from Küçükçekmece Lagoon. These results represent the first continuous paleomagnetic record from sediments over the last 3800 years, for northwestern Turkey, including a high temporal resolution relative geomagnetic field intensity record.

2. Materials and methods

2.1. Küçükçekmece Lagoon setting

The lagoon is situated 12 km north of the active northern branch of the North Anatolian Fault Zone (NAFZ), a transform plate boundary between the Eurasian and Anatolian plates. Küçükçekmece Lagoon (40.98°N, 28.76°E) is a brackish water lagoon located at the northern shoreline of the Sea of Marmara at the European part of İstanbul (Figure 1). It covers an area of 15 km^2, with a maximum depth of 20 m (Akçer Ön, 2011). The lagoon is connected to the Sea of Marmara via a 2 km long natural narrow channel. The main freshwater input is mainly from small streams and groundwater springs (Altun et al., 2009). The waters of the Ispartakule, Nakkaş and Sazlı streams are the main freshwater sources for the lake. The drainage basin of the lake covers an area of about 340 km^2, and its annual mean rainfall is 700 mm. The lake is surrounded by Lower Carboniferous sandstone, siltstone and shale, Eocene limestone to the north, Oligocene-Miocene sandstone, limestone and clay-bearing limestone to the west, and Miocene clay-bearing limestone with Eocene limestone to the east (Pehlivan and Yılmaz, 2004) (Figure 1).

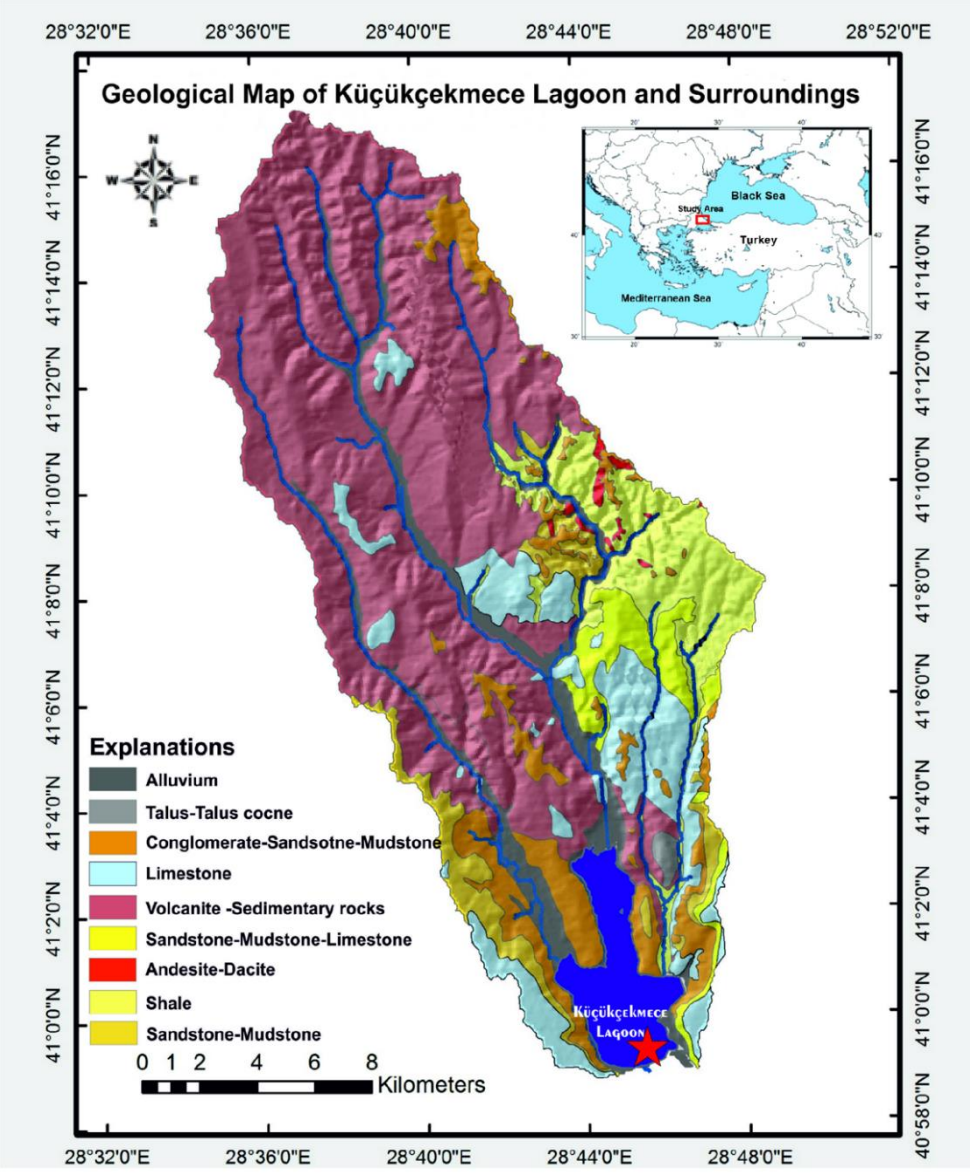

Figure 1. Geological map of the catchment area of Küçükçekmece Lagoon (Akçer Ön, 2011) and its location in NW Turkey. Red star shows coring location.

2.2. Cores and samples

Three piston cores, KCL12P1, KCL12P2, and KCL12P3, 10 cm in diameter, were recovered from varying depths between 17 m and 20 m from the southern part of Küçükçekmece Lagoon (Figure 1; Table 1). After their recovery, the cores were cut in the field into 1 m sections for transport to the core analysis laboratory in EMCOL (Eastern Mediterranean Centre for Oceanography and Limnology). All cores were stored in a 4 °C cold room until the measurements. In the laboratory, the cores were split into two halves, logged, described and sampled for various analyses.

2.3. XRF core-scanner elemental analysis

An Itrax X-ray fluoresence (XRF) core scanner equipped with XRF-EDS (energy-dispersive X-ray spectroscopy) was used for µ-XRF core scanner analysis at the EMCOL, İstanbul Technical University (Thomson et al., 2006). The archive core halves were scanned for elemental analysis at 60 µm and 1 mm resolution. Semi-quantitative elemental concentrations were recorded as counts per second (cps).

2.4. Dating and tuning

Total organic carbon (TOC) and plant fractions from three samples in core KCL12P2 were used for accelerator mass spectrometry (AMS) ^{14}C dating. The analyses were performed at the Poznań Radiocarbon Laboratory, Poland. ^{14}C ages were calibrated into calendar ages using the Calib 7.1 radiocarbon tools with the INTCAL09 calibration curve (Reimer et al., 2009) (Table 2).

XRF-Ca data, in addition to the AMS radiocarbon dates, were used for tuning to global proxies to create an age model. A particular graphics program, the comprehensive tool for correlation (xtc, Linux-based) developed at the Helmholtz Centre, German Research Centre for Geosciences (GFZ) Potsdam, Germany, was used for tuning. For dating purposes, newly acquired data sets are correlated to suitable time series, serving as master records. The deviation of the tuned age model from the preliminary linear model is usually less than the radiocarbon dating errors including reservoir effect (Avşar et al., 2014). The geochemical record (XRF Ca-counts) from the lagoon was tuned to the $\delta^{18}O$ record from Sofular Cave (Fleitmann et al., 2009), which is sited just 200 km from the lagoon. AMS C^{14} dates were used for an initial age model, which was then refined by the correlation of the Küçükçekmece Carecord to the Sofular oxygen isotope record at high resolution.

2.5. Paleo-rock magnetic measurements

A total of 714 oriented samples were taken with cubic plastic boxes with a volume of 6.0 cm^3 with 1 cm intervals. The subsampling was performed at the Yılmaz İspir Paleomagnetic Laboratory in İstanbul University-Cerrahpaşa and EMCOL, İstanbul Technical University.

All measurements of rock and paleomagnetic parameters, comprising low-field magnetic volume susceptibility (κ_{LF}), natural remanent magnetisation (NRM), anhysteretic remanent magnetisation (ARM), isothermal remanent magnetisation (IRM) and stepwise alternating field (AF) demagnetisation of the samples, were performed at the Laboratory for Paleo- and Rock Magnetism at Helmholtz Centre GFZ, Potsdam, Germany. Magnetic susceptibility (κ_{LF}) of all discrete samples was measured with an AGICO Kappabridge susceptibility meter to estimate the concentration of ferri-magnetic minerals within the samples. A 2G Enterprises 755 SRM long-core magnetometer with in-line and AF demagnetizer was used to identify the stable NRM directions and remove secondary viscous overprints at ten steps from 5 to 100 mT. Determination of the characteristic remanent magnetisation (ChRM) and the maximum angular deviation (MAD) for all samples was achieved by using principal component analysis (Kirschvink, 1980), calculated for successive measurements after AF demagnetisation from 15 to 65 mT. Relative paleointensity (rPI) variations were estimated from the slope of NRM versus ARM intensity of common demagnetization steps. Relative paleointensity (rPI) was estimated from the slope of NRM versus ARM

Table 1. The studied cores in Küçükçekmece Lagoon.

Core name	Location	Water depth (m)	Core length (cmblf)	Number of samples
KCL12P1	40°59′24.86″N 28°45′ 2.16″E	20	500	250
KCL12P2	40°59′24.86″N 28°45′ 2.16″E	20	513	176
KCL12P3	40°59′19.08″N 28°45′50.50″E	16	484	173

Table 2. Küçükçekmece Lagoon AMS radiocarbon data.

Core	Lab Code Poz #	Depth (cmblf)	Remark	Uncalibrated AMS ^{14}C age [a] (yr BP)	Calibrated AMS ^{14}C age [b] (yr BP)
KCL12P2	62291	66	Plant remains (0.6 mgC)	515 ± 35	529 ±16
	62293	138	Mud (TOC)	995 ± 30	894 ± 62
	62295	231	Mud (TOC)	1260 ± 30	1221 ± 41

[a] Uncalibrated ^{14}C age from total organic carbon and plant remain; [b] Calibrated ^{14}C age calculated using Calib 7.1 Program.

demagnetization steps, generally from 20 to 50 mT for the application of linear regression because, here, the trend mainly was linear with intercept values around zero. Choosing this interval ensures that the same portions of the coercivity spectrum from both the NRM and the ARM intensities are providing to the estimate of rPI (e.g., Levi and Banerjee 1976; Tauxe 1993; Valet 2003). An isothermal remanent magnetisation (IRM) was imparted using a 2G Enterprises 660 pulse magnetizer in a static peak field of 1.5 T (Saturation of IRM) and a reversed field of –0.2 T. S-ratio was calculated using the formula: $S = 0.5\times(1-(IRM_{-0.2T}/SIRM_{1.5\ T}))$, with $0\leq S\leq 1$ (after Bloemendal et al., 1992). If the S-ratio is close to 0, samples are dominated by high-coercivity magnetic minerals (e.g., hematite and goethite); whereas, values relative to 1 indicate that samples are dominated by low-coercivity minerals, such as magnetite (Fe_3O_4) and greigite (Fe_3S_4). To further identify magnetic mineralogy for selected samples, the Curie-Temperatures (T_C) were determined with a Kappabridge MFK1-FA in combination with a CS-3 unit and hysteresis parameters (coercive force H_C, coercivity of remanence H_{CR}, saturation magnetization M_S, and saturation remanence M_{SR}) were acquired using an alternating gradient magnetometer (AGM 3900) with a maximum field of 1 T, respectively. The hysteresis parameters (H_{CR}/H_C and M_{SR}/M_S) were plotted on a Day plot to determine the domain state of magnetic minerals (Day et al., 1977; Dunlop 2002).

3. Results and discussion

3.1. Sedimentology, core correlation and chronology

According to the lithological description, the cores comprise sediments deposited without any discontinuity and are composed of mainly light-grey, grey-brown colored laminated clay, intercalated by homogeneous black and homogeneous grey sediment layers (Figure 2). These distinctive layers were also used for correlation and the tuning process of the cores, based on lithological properties, besides mineral magnetic parameters, mainly high-resolution records of magnetic susceptibility and S-ratio. The down-core profiles of these parameters and the lithology of cores are highly comparable. A coherent correlation between the three studied cores showed that sediments being deposited in the same basin include comparable sediments; therefore, they are useful to stack paleomagnetic data. A mean sedimentation rate of 0.18 cm/yr was derived from KCL12P2, supporting the construction of a high-resolution paleomagnetic paleosecular variation record.

The age model of Küçükçekmece Lagoon sediments is based on three calibrated radiocarbon dates obtained from core KCL12P2 (Table 2) and tuning of the geochemical record of core KCL12P2 to the $\delta^{18}O$ record from Sofular Cave (Fleitmann et al., 2009) (Figure 3). Many studies showed that the Sofular Cave record is very significant for the creation of age models and the interpretation of paleoclimate variations (Avşar et al., 2014; Çağatay et al., 2019; Makaroğlu et al., 2020). The $\delta^{18}O$ record mainly reflects regional/global features; whereas, the $\delta^{13}C$ record can be masked by local signals (Hercman et al., 2020). Therefore, the $\delta^{18}O$ record was used instead of the $\delta^{13}C$ record from Sofular Cave in this study. There are striking similarities between the Küçükçekmece Lagoon sediment parameter (XRF Ca-counts) and the Sofular oxygen isotope record, which helped to create a high-resolution age model for studied sediments (Figure 3). According to the age-depth model of core KCL12P2, the sediment covers the last 3800 years (Figure 3). The other two cores, KCL12P1 and KCL12P3, were tuned using magnetic susceptibility and S-ratio records from KCL12P2, which were dated at high-resolution.

3.2. Mineral magnetic properties

Mineral magnetic properties indicating magnetic mineral concentration, hysteresis data, thermomagnetic and remanent variations of the cores from Küçükçekmece Lagoon are shown in Figures 2, 4, 5, and 6, respectively. According to the rock magnetic properties, the cores visually consist of three different magnetic units (1 to 3). Unit 1, which is the typical lithology for Küçükçekmece Lagoon sediments, shows a relatively moderate and stable magnetic susceptibility and S-ratio values throughout the cores with an average of 80×10^{-6} and 0.95, respectively (Figure 2). Unit 3 shows relatively low S-ratio values indicating an increase in high coercivity (or decrease in low coercivity) magnetic minerals in all studied cores except core KCL12P3, taken from a different location than KCL12P1 and KCL12P2 (Figure 2). Laminated and homogeneous sediments from units 1 and 3 are characterized by pseudo-single domain particles, low magnetic moment and weak hysteresis loops (Figures 4a, 4c), which is saturated below 0.3 T, indicating low coercivity magnetic minerals (Figure 4c). S-ratio variations in Kücükçekmece lagoon sediments, ranging from 0.95 to 1, indicate that the sediments include low coercivity magnetic minerals (e.g., magnetite). This is also supported by other rock magnetic properties, such as low MDF values. Low MAD values indicate a stable paleomagnetic direction record (Figure 6). The values of M_{RS}/M_S and H_{CR}/H_C plotted in a day diagram indicate that the magnetic mineralogy of the lagoon sediments from unit 3 is dominated by pseudo single-domain (PSD) particles, similar to the sediments from unit 1 (Figure 4a). In thermomagnetic curves, the major decrease in magnetic susceptibility is at about 580 °C, indicating the presence of magnetite for both units, while the significant increase after 200 °C probably indicates the formation of a new magnetic phase from clay minerals (Figure 5c). The heating curves from unit 1 also indicate the chemical transformation of clay minerals into a new magnetic phase (Roberts, 2015). The formation of new magnetic phase (e.g., magnetite) is supported by the cooling curves; the steep increase in susceptibility from 580 to 300 °C shows the mineralogical transformation of the paramagnetic minerals during the heating stage (Hrouda, 1994; Sagnotti et al., 1998).

High $SIRM/\kappa_{LF}$ values above 10 kAm^{-1} recovered from the lake and marine sediments clearly indicate secondary

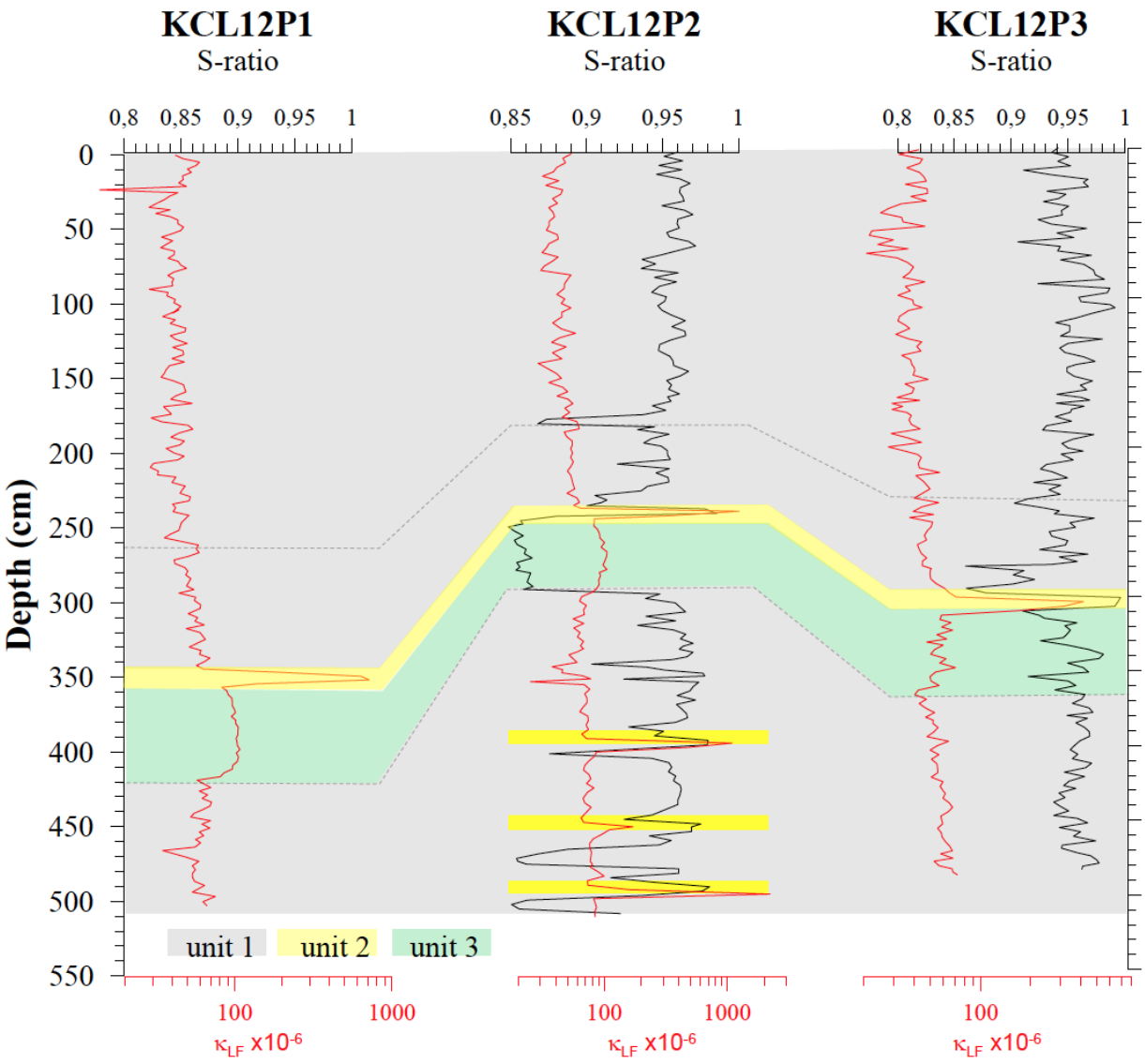

Figure 2. Down-core magnetic susceptibility (κ_{LF}) and S-ratio profiles for cores KCL12P1, KCL12P2 and KCL12P3. Dashed lines indicate main correlative features. Yellow bars represent homogeneous black layers containing significant amounts of greigite.

magnetic minerals such as greigite (Snowball and Thompson, 1990; Snowball, 1991; Roberts and Turner, 1993; Reynolds et al., 1994; Ron et al. 2007; Roberts, 2015). The highest κ_{LF} values (15 – 223×10^{-6}), S-ratios (0.95–1), and SIRM/κ_{LF} ratios (20–100 kAm^{-1}) indicate that the secondary diagenetic iron sulphide (e.g., greigite) is the dominant magnetic mineral in homogenous black sediments, which is defined as unit 2 (Figure 2). The stratigraphic positions of these samples are evidenced by a high SIRM/κ_{LF} ratio between 15 and 100 kAm^{-1} (Figure 6). Such high values are considered to be indicative of the secondary magnetic iron sulphide minerals also by previous studies (e.g., Snowball, 1991; Roberts and Turner, 1993; Nowaczyk et al., 2012, 2013). The hysteresis parameters support that unit 2 is also dominated by single domain (SD) greigite causing characteristic distinctive peaks, varying between 10 and 5 cm in thickness marked by yellow bars in Figure 2. Hysteresis curves of greigite samples show wide loops and a strong magnetic moment, (Figure 4b). Greigite layers were found at various depths of 250, 390, 450, and 490 cm in core KCL12P2, while there were found just two layers in cores KCL12P1 and KCLP3 with the depths of 350 cm and 300 cm, respectively (yellow bars in Figure 2). The thermomagnetic curve of samples from unit 2 showed typical behavior of greigite, with decreasing magnetic susceptibility at the temperature of around 380 °C (Figure 5c). Magnetic susceptibility can show a temporal increase above ~250 °C, being typical for greigite-bearing samples (e.g., Roberts and Turner, 1993) as observed in Küçükçekmece sediments (Figure 5c).

3.3. Quality of paleomagnetic data

The studied cores comprise a continuous sediment sequence without any gaps, which allows recovering a high-resolution and continuous paleomagnetic record

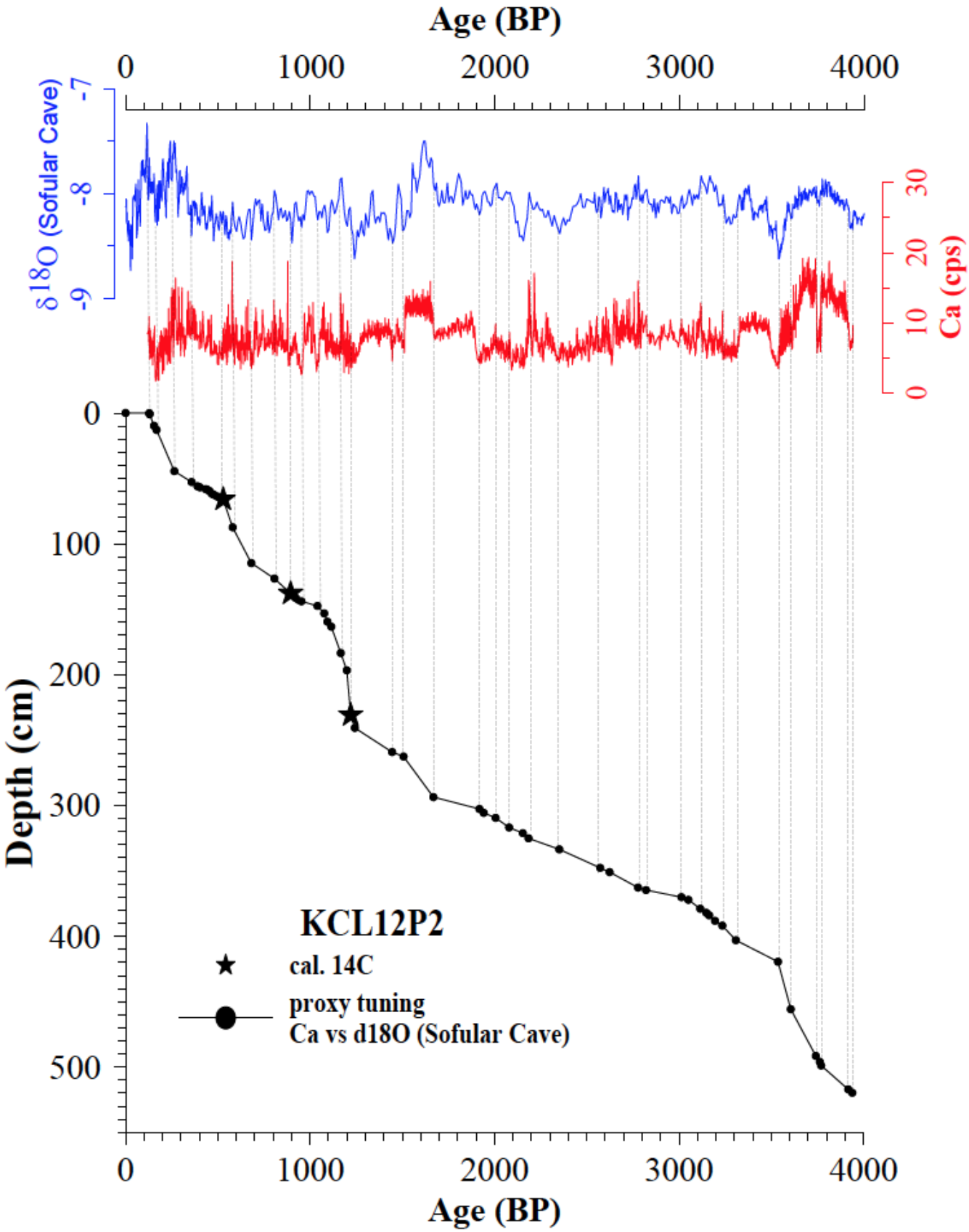

Figure 3. Age-depth model for core KCL12P2 recovered from the deepest part of the lagoon based on radiocarbon dating (cal.^{14}C) and proxy tuning (XRF Ca-counts vs δ^{18}O (Fleitmann et al., 2009). Radiocarbon dates were used as initial tie points for the age model.

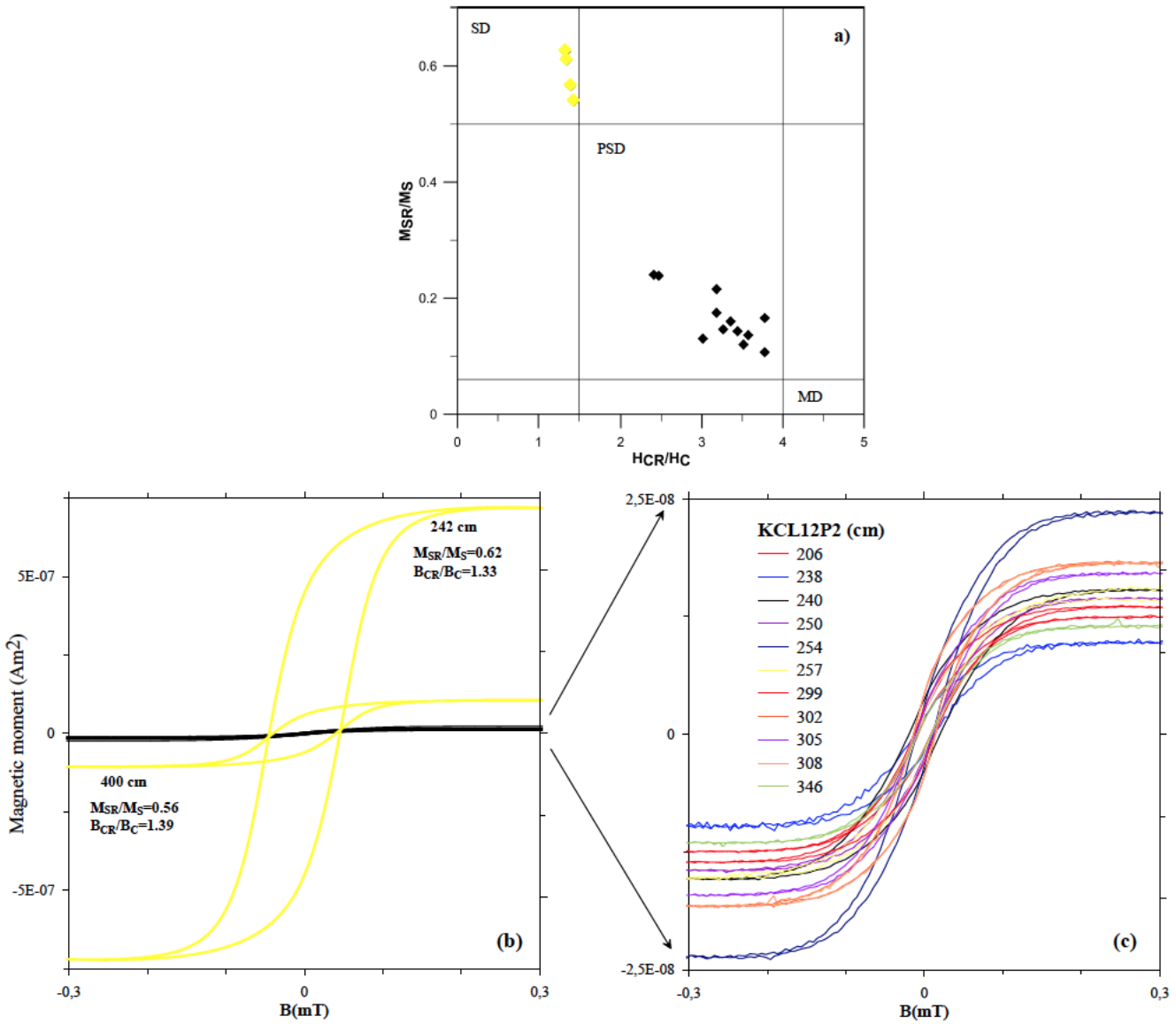

Figure 4. Day plot (Day et al. 1977) (a) and hysteresis properties (b, c) of representative samples from core KCl12P2. Yellow lines and diamonds indicate results from greigite-bearing sediments from Küçükçekmece Lagoon.

from the lagoon. According to thermo-magnetic properties, Küçükçekmece Lagoon sediments consist of low coercivity magnetite, which has a typical Curie point indicated by a sharp decrease at 580 °C (Figure 5c). The temperature dependence of magnetic susceptibility is complicated to interpret because the paramagnetic matrix minerals significantly contribute to potentially weak ferri-magnetic compounds such as in lake sediments at low applied fields (Hrouda, 1994: Roberts et al., 2011). Thermo-magnetic analyses also showed that Küçükçekmece Lagoon sediments contain higher amounts of paramagnetic minerals than ferro-magnetic particles except for the homogenous black layers, containing high amounts of greigite. Hysteresis data from the selected samples indicate that low coercivity minerals such as magnetite are the dominant magnetic carriers within the studied sediments, characterized by pseudo-single domain behavior (Figure 4).

According to their mineral magnetic properties, Küçükçekmece Lagoon sediments are characterized by low-coercivity magnetic minerals with low MAD values (Figure 6). The data obtained from the greigite-bearing samples, which are found in unit 2 were eliminated from paleomagnetic records. Therefore, the paleomagnetic data obtained from Küçükçekmece lagoon sediments are suitable to provide a high-resolution paleomagnetic secular variation record for NW Turkey (Figures 7, 8).

3.4. Paleomagnetic directions and paleointensity

All samples with SIRM/κ_{LF} values > 10 kAm^{-1} and S-ratios > 0.95 were interpreted as contaminated by secondary magnetic iron sulphides, namely greigite (indicated by yellow diamonds in Figure 6). Therefore, they were excluded from further processing of paleomagnetic data.

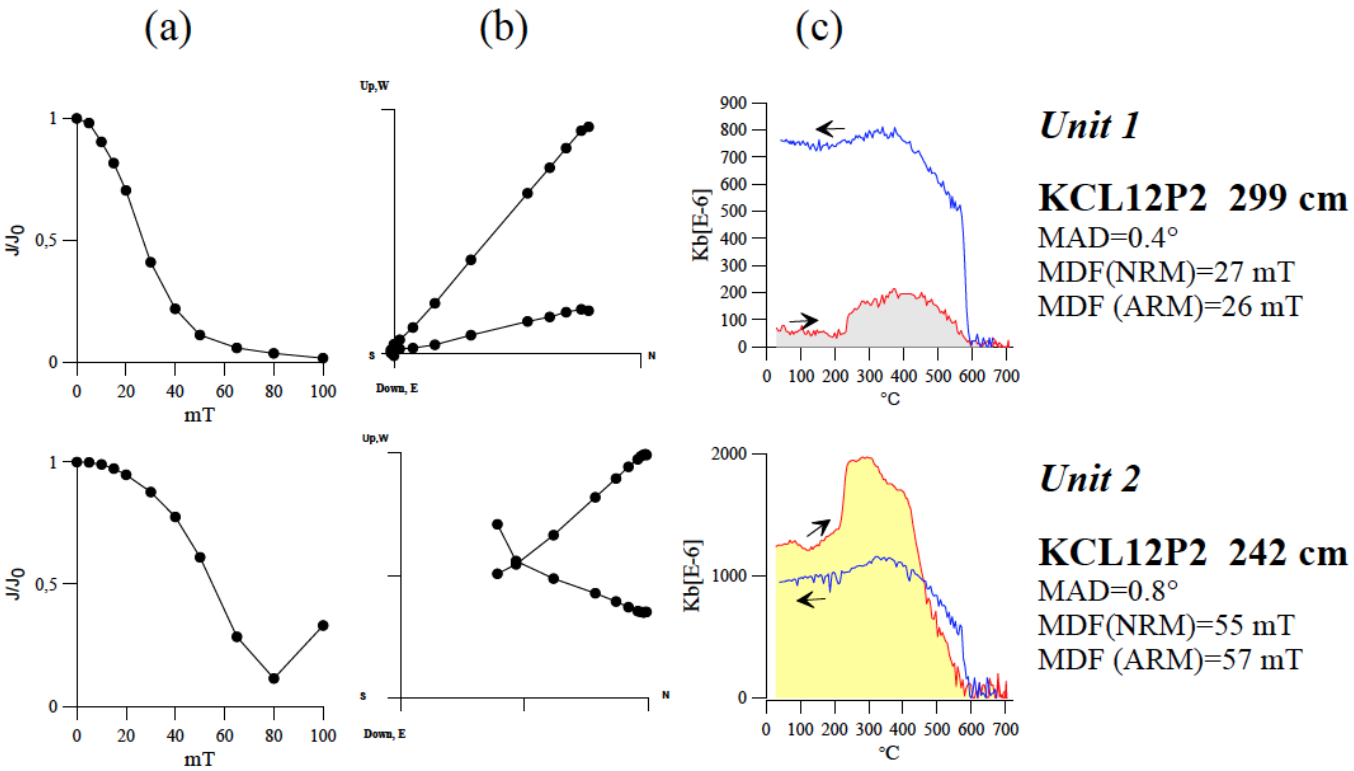

Figure 5. Alternating field demagnetization results (a), Zijderveld diagrams (b) and thermo-magnetic experiment results (c) from selected samples from core KCL12P2. MAD (maximum angular deviation), MDF (Median Destructive Field). In c) red (blue) marks the heating (cooling) curve.

Low MDF values varying between 25 to 27 mT indicate that these samples are dominated by low-coercivity magnetic minerals such as magnetite (Figure 6), while high MDF values of up to 100 mT are related to greigite. MAD values of all studied samples are mostly < 5°, indicating stable ChRM directions due to a relatively high concentration of low-coercivity magnetic minerals (e.g., magnetite) in the pseudo-single domain range and a high detrital input.

Results from alternating field demagnetization shown as vector component diagrams (Zijdervelt, 1967) from representative Küçükçekmece Lagoon sediment samples are shown in Figures 5a, 5b. There are two groups of vector component behavior for the samples from Küçükçekmece Lagoon. Figure 5 shows the directional variation of two selected samples during AF demagnetization. A small viscous remanent magnetization was removed at 10 to 15 mT AF peak amplitude. It clearly appears that almost all samples, except gregite-bearing samples, carry a single paleomagnetic direction demagnetized between 10 and 80 mT, with vector endpoints migrating towards the origin (Figure 5). The maximum angles of deviation (MAD angles) of less than 5° also reflect this stable characteristic remanence (Figure 6). The second type of samples, which are dominated by greigite, don't migrate towards the origin (Figure 5). In contrast, this type of samples acquired a gyro-remanent magnetisation (GRM) after 65 mT. This AF demagnetization behavior is typical for greigite-bearing sediments, usually found in the lake and marine sediments (Roberts et al., 2011). The presence of greigite compromises the paleomagnetic records, thus, requiring the data to be filtered from its influence. In this study, the data obtained from greigite samples, which were found in unit 2, were eliminated (Figures 2, 5, and 6).

Directional data of ChRM inclination and declination obtained from three studied cores exhibit typical secular variation patterns (Figures 6, 7). For the study area, the inclination expected from a geocentric axial dipole (GAD) is 60°. The obtained mean inclination value (50°) of the cores is very close to the GAD inclination, whereas the upper part of the cores, between about 0 and 50 cm, exhibit shallower inclinations. Shallow magnetization directions, which are very common in freshwater lake sediments, can be caused by compaction, sediment disturbance during deposition, sampling, drilling and recovery (Marco et al., 1998; Channell et al., 2020). These shallow inclinations, found in the top 50 cm of the cores, are likely caused by not yet unconsolidated or "soupy" mud. However, some other low inclinations intervals are related with paleosecular variations, which are a typical pattern for the Holocene period (Korte et al., 2011). The declination records from studied cores are characterized by some larger swings (about 40 ◦) than expected patterns in the depths of 230, 250, and 200 cm in cores KCL12P1, KCL12P2, and KCL12P3, respectively. These swings could be recorded due to a possible rotation of this interval or a small break in the sediment.

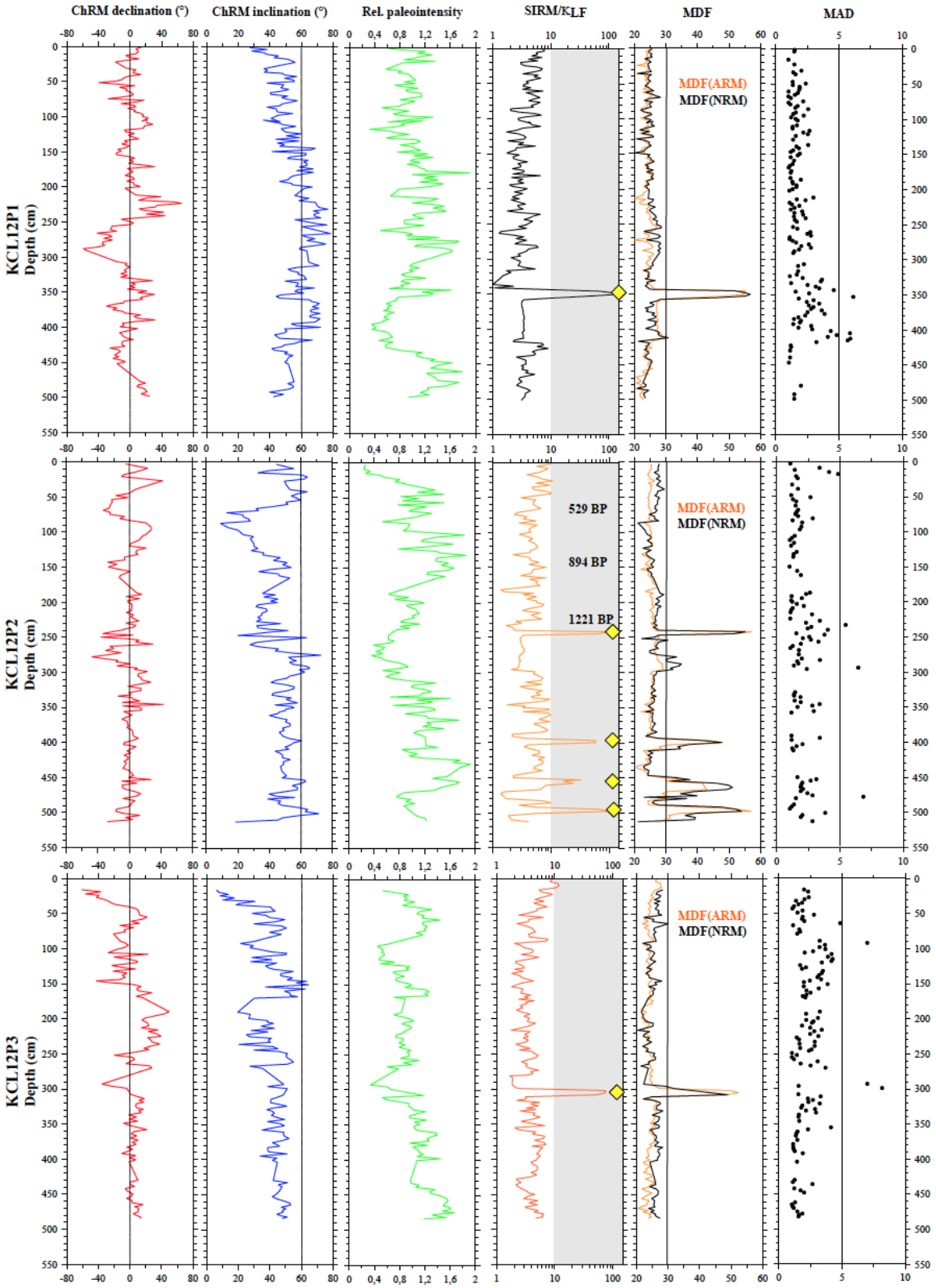

Figure 6. Down-core variation of paleomagnetic directions (ChRM declination, ChRM Inclination), relative paleointensity (rPI) derived from the slope of NRM versus ARM, and magnetic minerology (S-ratio) from cores KCL12P1, KCL12P2, and KCL12P3. Grey bars indicate the influence of secondary magnetic minerals. Yellow diamonds denote the presence of greigite (see also yellow markings in Figures 2, 4a, b, 5c). MAD - maximum angular deviation, MDF - median destructive field, ChRM - characteristic remanent magnetisation. The inclination ±60 and declination (0, 180), as expected for a geocentric axial dipole direction are shown by the vertical dashed lines in the directional plots.

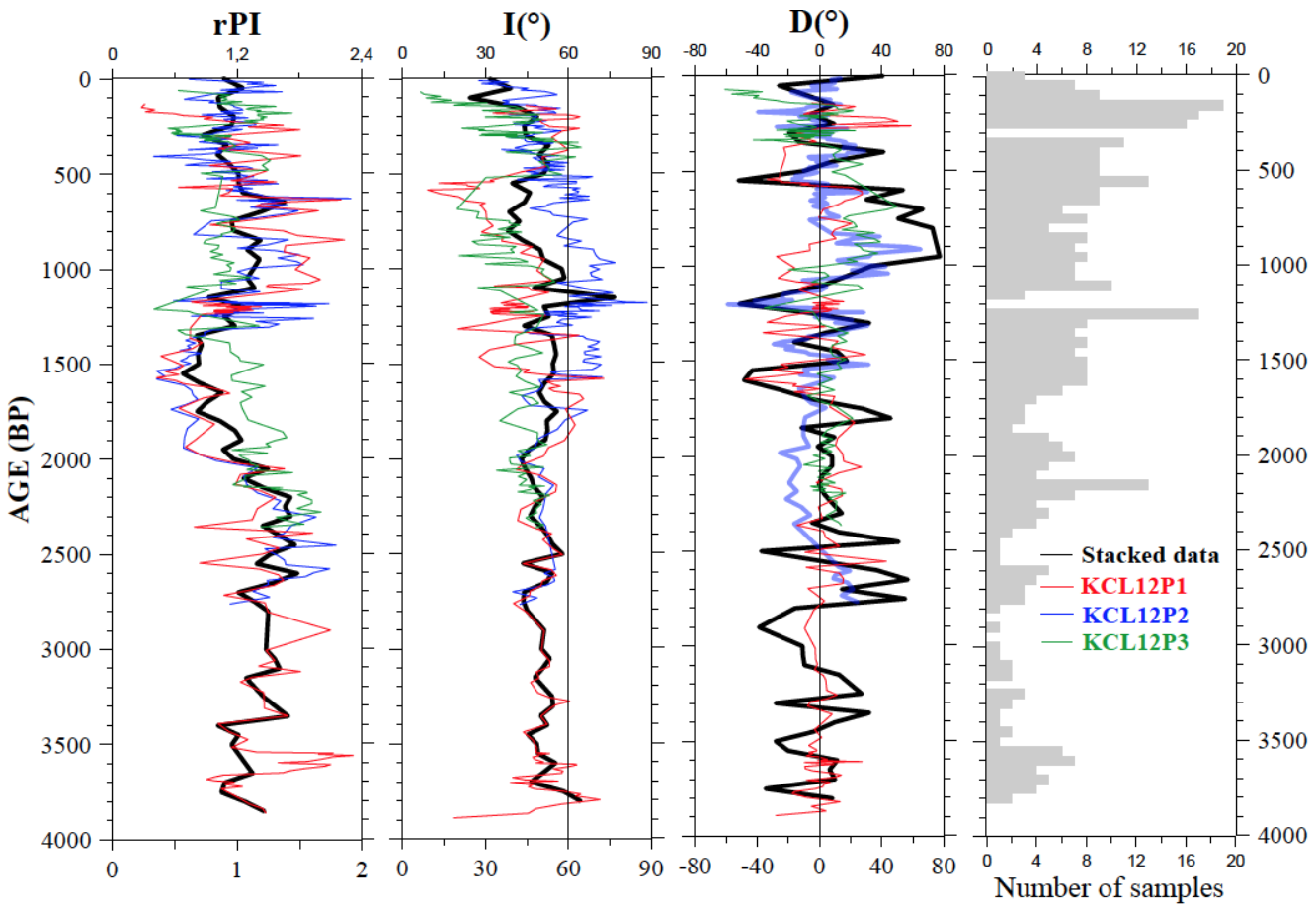

Figure 7. The relative paleointensity (rPI) and paleomagnetic directions (I, D) of studied cores and the stacked data (black lines). Grey bars show the number of samples used for stacking into 50 years bins.

Relative paleointensity (rPI) records from the studied cores versus depth are shown in Figure 6. rPI variations of the studied cores also show PSV patterns similar to the directional data. The stacked ChRM directions (I, D) and associated relative paleointensity variations from Küçükçekmece Lagoon sediments are shown in Figure 7. To obtain a paleomagnetic data stack from the continuously deposited sediments of the last 3800 years, 50 yr bins were used. The number of samples per time bin of the stacked PSV record is shown by the histogram in the right panel of Figure 7. For the time between 2400 and 100 years, BP, the number of samples per time bin lies mainly between 4 and 18, while older time bins are based on fewer samples, between 0 and 4. After greigite filtering, few data were left from the samples older than 2000 a. BP. The high data density in the interval from 2000 a. BP to present is due to reliable paleomagnetic directions and high amounts of low-coercivity magnetic mineral assemblages interpreted to be carried by magnetite, whereas the lower data density is due to greigite-bearing sediments, mainly found in the bottom parts of the cores deposited between 2000–3800 a, BP (Figure 7).

3.5. Comparison of the paleomagnetic record from Küçükçekmece Lagoon with the regional record

The high-resolution paleomagnetic record for NW Turkey for the last 3800 a. BP is shown in Figures 7. The average sedimentation rate derived from the cores is 0.18 cm/year on average. This means that a ~3 cm interval (the size of a paleomagnetic sample) covers ~16 years. Thus, the obtained data provide a high-resolution paleomagnetic record for the region. Figure 8 shows a comparison of the Küçükçekmece paleomagnetic records with data from the Sea of Marmara (Makaroğlu et al., 2020) and geomagnetic models (Korte et al.,2009; Korte and Constable, 2011; Korte et al.,2011; Brown et al., 2015). Comparison of Küçükçekmece and the Sea of Marmara paleomagnetic records does not show a good agreement for the last 2500 years. This is likely due to observed core disturbances in the upper 2 m part of the Marmara core as Makaroğlu et al. (2020) presented. However, the older parts of the two records show similar paleointensity variations, inclinations and declinations (Figure 8). Inclination values from Küçükçekmece Lake sediments from the last 3800 years are shallower than the regional models and paleomagnetic directions obtained from archeological artifacts (Ertepınar et al., 2012) and volcanic rocks (Kaya, 2020) in this area. High sedimentation rates with the observed detrital siliciclastic and iron oxide inputs could be the cause of these shallow inclinations, as shown in many lakes and marine sediments (Makaroğlu et al., 2020). Comparison of the Küçükçekmece paleomagnetic record (rPI, I, D) with the high-resolution regional model

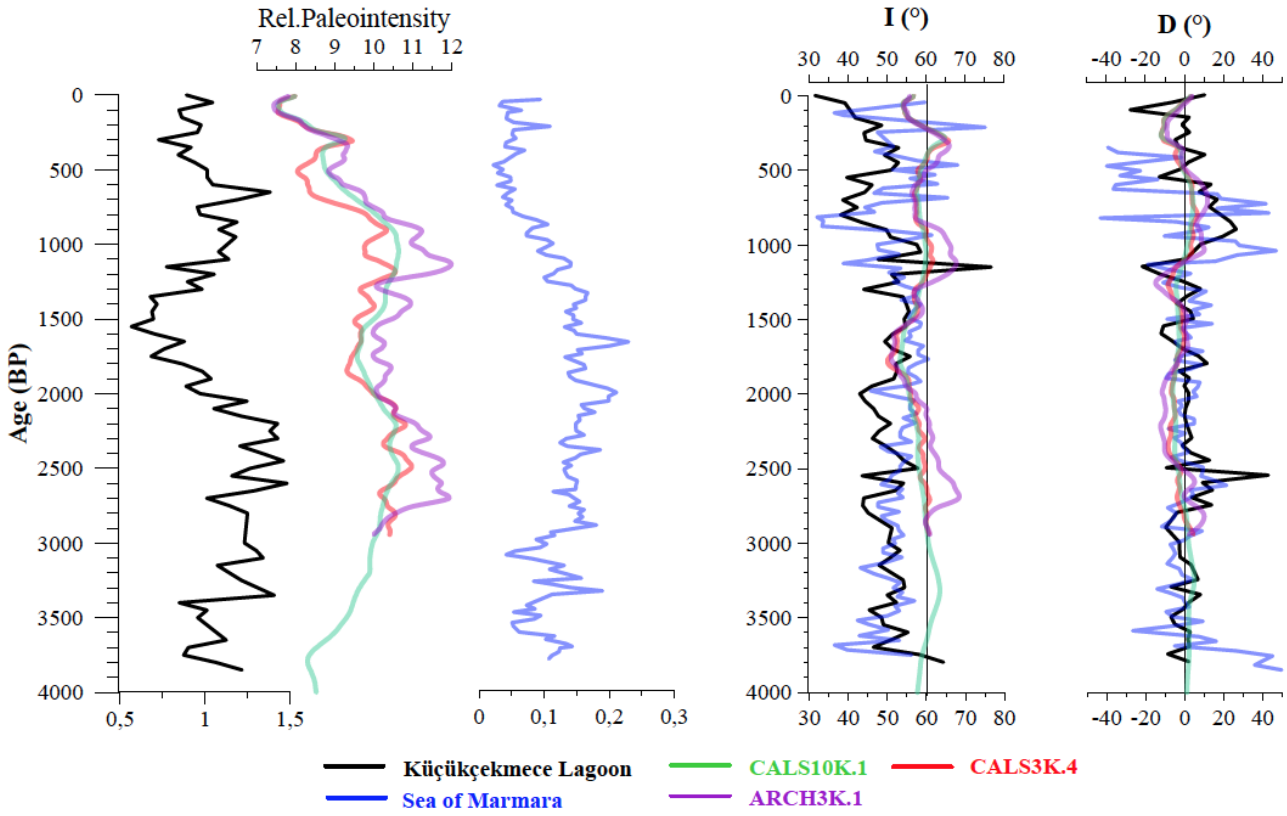

Figure 8. Comparison of Küçükçekmece Lagoon paleomagnetic records (black lines) with data from the Sea of Marmara (blue lines, Makaroğlu at al., 2020) and geomagnetic models CALS10K.1 (Korte et al., 2011), CALS3K.4 (Korte and Constable, 2011), ARCH3K.1 (Korte et al., 2009). All field model data were downloaded from the GEOMAGIA50.v3.4 data base (Brown et al., 2015).

records, which have been recently developed using field models based on compilations of archaeomagnetic (ARCH3K.1) (Korte et al., 2009), lake sediment data (CALS3k.4) (Korte and Constable, 2011) and CALS10k.1 (Korte et al., 2011) show a good agreement and similar variation patterns as seen in Figure 8. The shallow inclination values in the Küçükçekmece lagoon record between 600–800 years BP, as seen in Figure 8 is remarkable. These low values obtained from Küçükçekmece are also compatible with the ones from the Sea of Marmara (Makaroğlu et al., 2020; Drab et al., 2015) and global data, which also show low inclinations between 600–800 years BP. However, the inclination values from Küçükçekmece Lagoon are shallower than these records. Declination variation shows a similar pattern with the data obtained from the Sea of Marmara and curves calculated from global models (Figure 8).

4. Conclusion

This study provides a new paleosecular variation record including paleointensity and paleomagnetic directional data (inclination, declination) from Küçükçekmece Lagoon, located in NW Turkey. According to the age-depth model based on radiocarbon dating and global proxy tuning, the record covers the last 3800 years. The correlation of stacked directional data and relative paleointensity variations from Küçükçekmece sediment cores with regional geomagnetic models shows a good agreement. This correlation reveals a striking similarity between the data from Küçükçekmece Lagoon and those from the surrounding region over the last 3800 years. A low inclination period between 600–800 years BP and low paleointensity around 1500 BP are quite remarkably similar patterns observed for all of these different areas.

The data obtained in this work for the last 3800 years provide a significant data set that can be fed into a future master paleosecular variation for Turkey. Creating such a master curve will provide an important dating tool for future studies in Turkey. The new high-resolution paleomagnetic data from Küçükçekmece Lagoon are useful especially for the late Holocene period. However, it is also recommended to increase the number of such records from nearby regions by further studies in order to constrain better and to extend the data from the current study further back in time.

Acknowledgments

This work was supported by İstanbul University-Cerrahpaşa Scientific Research Foundation (Project numbers: 22799, 45018, 41415, 30199, 23013). I would like thank Norbert Nowaczyk for his support in the GFZ paleomagnetic Laboratory, contribution to the

manuscript and delightful discussions. I thank Namık Çağatay, Sena Akçer Ön, and Z. Bora Ön for comprehensive comments to the manuscript. I thank Dursun Acar for XRF analysis and his help during the coring campaign, Nurcan Kaya, Melda Küçükdemirci, Umut Barış Ülgen, and Mehmet Makar for their support during sampling and coring. I also thank the editor and three anonymous reviewers for their constructive comments, which improved the manuscript.

References

Akçer Ön S (2011). Küçükçekmece Lagünü, Yeniçağa, Uludağ Buzul Ve Bafa Gölleri'nin (Batı Türkiye) Geç Holosen'deki İklim Kayıtları: Avrupa Ve Orta Doğu İklim Kayıtları İle Karşılaştırılması. PhD, İstanbul Technical University, İstanbul, Turkey (in Turkish).

Altun Ö, Saçan MT, Erdem AK (2009). Water quality and heavy metal monitoring in water and sediment samples of the Küçükçekmece Lagoon, Turkey (2002–2003). Environmental Monitoring and Assessment 151: 345–362. doi: 10.1007/s10661-008-0276-8

Anker S, Colhoun E, Barton C, Peterson M, Barbetti M (2001). Holocene Vegetation and Paleoclimatic and Paleomagnetic History from Lake Johnston, Tasmania. Quaternary Research. 56, 264-274. doi:10.1006/qres.2001.2233

Avşar U, Hubert-Ferrari A, Batist M, Fagel N (2014). A 3400 year lacustrine paleoseismic record from the North Anatolian Fault, Turkey: Implications for bimodal recurrence behavior, Geophysical Research Letter 41: 377–384. doi: 10.1002/2013GL058221

Bloemendal J, King JW, Hall FR, Doh SH (1992). Rock magnetism of late Neogene and Pleistocene deep-sea sediments: Relationship to sediment source, diagenetic processes, and sediment lithology. Journal of Geophysical Research 97: 4361–4375. doi: 10.1029/91JB03068

Brandt U, Nowaczyk NR, Ramrath A, Brauer A, Mingram J et al. (1999). Palaeomagnetism of Holocene and Late Pleistocene sediments from Lago di Mezzano and Lago Grande di Monticchio (Italy): initial results. Quaternary Science Reviews 18: 961-976.

Brown MC, Donadini F, Korte M, Nilsson A, Korhonen K, Lodge A. Lengyel SN, Constable CG (2015). GEOMAGIA50.v3: 1. General structure and modifications to the archeological and volcanic database. Earth Planets Space 67:83. doi: 10.1186/s40623-015-0232-0

Çağatay MN, Uçarkuş G (2019). Morphotectonics of the Sea of Marmara: basins and highs on the North Anatolian continental transform plate boundary. In: João C. Duarte (editor). Transform Plate Boundaries and Fracture Zones, Chapter 16, pp. 397–415. doi: 10.1016/B978-0-12-812064-4.00016-5

Channell JET, Singer BS, Jicha BR (2020). Timing of Quaternary geomagnetic reversals and excursions in volcanic and sedimentary archives. Quaternary Science Reviews. 228: 106114. doi: 10.1016/j.quascirev.2019.106114.

Day R, Fuller M, Schmidt VA (1977). Hysteresis properties of titanomagnetites: grain-size and compositional dependence, Physics of the Earth and Planetary Interiors 13: 260-267. doi: 10.1016/0031-9201(77)90108-X

Drab L, Carlut J, Hubert-Ferrari A, Martinez P, LePoint G et al. (2015). Palaeomagnetic and geochemical record from cores from the Sea of Marmara, Turkey: age constraints and implications of sapropelic deposition on early diagenesis, Marine Geology 360: 40–54. doi: 10.1016/j.margeo.2014.12.002

Dunlop DJ (2002). Theory and application of the Day plot (M-rs/M-s versus H-cr/H-c) 1. Theoretical curves and tests using titanomagnetite data. Journal of Geophysical Research 107(B3): 2056. doi: 10.1029/2001JB000486

Ertepınar P, Langereis CG, Biggin AJ, Frangipane M, Matney T et al. (2012). Archaeomagnetic study of five mounds from upper Mesopotamia between 2500 and 700BC: further evidence for an extremely strong geomagnetic field ca. 3000 years ago. Earth and Planetary Science Letters 357: 84–98. doi: 10.1016/j.epsl.2012.08.039

Ertepınar P, Langereis CG, Biggin AJ, de Groot LV, Kulakoğlu F et al. (2016). Full vector archaeomagnetic records from Anatolia between 2400 and 1350 BCE: implications for geomagnetic field models and the dating of fires in antiquity. Earth and Planetary Science Letters. 434: doi: 171–186. 10.1016/j.epsl.2015.11.015

Ertepınar P, Hammond ML, Hill MJ, Biggin AJ, Langereis CG et al. (2020). Extreme geomagnetic field variability indicated by Eastern Mediterranean full-vector archaeomagnetic records. Earth and Planetary Science Letters 531: 115979. doi: 10.1016/j.epsl.2019.115979

Fleitmann D, Cheng H, Badertscher S, Edwards RL, Mudelsee M et al. (2009). Timing and climatic impact of Greenland interstadials recorded in stalagmites from northern Turkey. Geophysical Research Letters 36: 19707. doi: 10.1029/2009GL040050

Frank U, Schwab MJ, Negendank JFW (2002). A lacustrine record of paleomagnetic secular variations from Birkat Ram, Golan Heights (Israel) for the last 4400 years. Physics of the Earth and Planetary Interiors 133: 21–34. doi: 10.1016/S0031-9201(02)00085-7

Frank U, Nowaczyk NR and Negendank JFW (2007). Palaeomagnetism of greigite bearing sediments from the Dead Sea, Israel. Geophysical Journal International 168: 904–920. doi: 10.1111/j.1365-246X.2006.03263.x

Gogorza CSG, Sinito AM, Vilas JF, Creer KM, Nunez H (2000). Geomagnetic secular variations over the last 6500 years as recorded by sediments from the lakes of south Argentina. Geophysical Journal International

143: 787– 798. doi: 10.1046/j.1365-246X.2000.00277.x

Haltia-Hovi E, Nowaczyk N, Saarinen T (2010). Holocene palaeomagnetic secular varition recorded inmultiple lake sediments cores from eastern Finland. Geophysical Journal International 180: 609–622. doi: 10.1111/j.1365-246X.2009.04456.x

Hercman H, Gaesiorowski M, Pawlak J, Błaszczyk M, Gradziński M et al. (2020). Atmospheric circulation and the differentiation of precipitation sources during the Holocene inferred from five stalagmite records from Demänová Cave System (Central Europe). The Holocene. 30 (6): 834. doi: 10.1177/0959683620902224

Hrouda F (1994). A technique for the measurement of thermal changes of magnetic susceptibility of weakly magnetic rocks by the CS-2 Apparatus and KLY-2 Kappabridge, Geophysical Journal International 118: 604-612. doi: 10.1111/j.1365-246X.1994.tb03987.x

Kaya N (2020). Orta ve Batı Anadolu'da Jeomanyetik Alan Şiddetinin Neojen-Kuvaterner boyunca Değişimi, PhD. İstanbul Üniversitesi-Cerrahpaşa, Yüksek Lisans Enstitüsü (in Turkish).

Kirschvink JL (1980). The least-squares line and plane and the analysis of palaeomagnetic data. Geophysical Journal International 62: 699–718. doi: 10.1111/j.1365-246X.1980.tb02601.x

Korfmann M, Becher H (1987). Demircihöyük, Die ergebnisse der Ausgrabungen 1975-1978, Philipp von Zabern and Mainz am Rhein. doi: 10.11588/ger.1990.61603

Korte M, Donadini F, Constable CG (2009). Geomagnetic field for 0–3 ka: 2. A new series of time-varying global models. Geochemistry Geophysics Geosystems (G3) 10: Q06008. doi: 10.1029/2008GC002297

Korte M, Constable C (2011). Improving geomagnetic field reconstructions for 0– 3 ka. Physics of the Earth and Planetary Interiors 188: 247–259. doi: 10.1016/j.pepi.2011.06.017

Korte M, Constable C, Donadinic F, Holmed R (2011). Reconstructing the Holocene geomagnetic field. Earth and Planetary Science Letters 312 (3-4): 497-505. doi: 10.1016/j.epsl.2011.10.031

Kotilainen AT, Saarinen T, Winterhalter B (2000). High-resolution paleomagnetic dating of sediments deposited in the central Baltic Sea during the last 3000 years. Marine Geology 166: 51–64. doi: 10.1016/S0025-3227(00)00012-8

Kovacheva M (1980). Summarised results of the archaeomagnetic investigations of the geomagnetic field variation for the last 8000 years in South-Eastern Europe, Geophysical Journal Royal Astronomical Society 61: 57-64. doi: 10.1111/j.1365-246X.1980.tb04303.x

Lapointe L, Francus P, Stoner JS, Abbott MB, Balascio, NL et al. (2019). Chronology and sedimentology of a new 2.9 ka annually laminated record from South Sawtooth Lake, Ellesmere Island. Quaternary Science Reviews 222: 105875. doi: 10.1016/j.quascirev.2019.105875

Ledu D, Rochon A., Vernal A, Barletta F, Onge G (2010). Holocene sea ice history and climate variability along the main axis of the Northwest Passage, Canadian Arctic. Paleoceanography 25: 2213. doi: 10.1029/2009PA001817

Levi S, Banerjee SK (1976). On the possibility of obtaining relative paleointensities from lake sediments. Earth and Planetary Science Letters 29: 219– 226. doi: 10.1016/0012-821X(76)90042-X

Makaroğlu Ö, Nowaczyk NR, Eriş KK, Çağatay MN (2020). High-resolution palaeomagnetic record from Sea of Marmara sediments for the last 70 ka. Geophysical Journal International. 222: 2024-2039. doi: 10.1093/gji/ggaa281

Makaroğlu Ö (2011). Van Gölü Sedimanlarının Çevre Mağnetizması ve Paleomağnetik Kayıtları. İstanbul.Üniversitesi. Fen Bilimleri Enstitüsü. PhD. (in Turkish)

Mensing SA, Schoolman EM, Tunno I, Noble P, Sagnotti L et al. (2018). Historical ecology reveals landscape transformation coincident with cultural development in central Italy since the Roman Period. Science Report 8: 2138. doi: 10.1038/s41598-018-20286-4

Marco S, Ron H, McWilliams MO, Stein M (1998). High-Resolution Record of Geomagnetic Secular Variation from Late Pleistocene Lake Lisan Sediments (Paleo Dead Sea). Earth and Planetary Science Letters 161: 145–160. doi: 10.1016/S0012-821X(98)00146-0

Mothersill JS (1996) Paleomagnetic results from LakesVictoria and Albert, Uganda. Studia Geophysica et Geodaetica 40: 25–35.

Nowaczyk NR, Arz HW, Frank U, Kind J, Plessen B (2012). Dynamics of the Laschamp geomagnetic excursion from Black Sea sediments. Earth and Planetary Science Letters 351–352: 54–69. doi: 10.1016/j.epsl.2012.06.050

Nowaczyk NR, Frank U, Kind J, Arz HW (2013). A high-resolution palaeointensity stack of the past 14 to 68 ka from Black Sea sediments. Earth and Planetary Science Letters 384: 1–16. doi: 10.1016/j.epsl.2013.09.028

Nilsson A, Holme R, Korte M, Suttie N, Hill M (2014). Reconstructing Holocene geomagnetic field variation: new methods, models and implications Geophysical Journal International 198: 229-248. doi: 10.1093/gji/ggu120

Nourgaliev D, Heller F, Borissov A, Iassonov P, Khassanov D et al. (2000). Paleomagnetism of recent Russian lake sediments. Geologica Carpathica 51: 179–180.

Pehlivan R, Yilmaz O (2004). Geochemistry and mineralogy of bottom sediments in the Kuçukçekmece Lake, Istanbul, Turkey. Geochemistry International 42: 1099–1106.

Ponat E (1995). Archaeomagnetism in Western Turkey, PhD, Boğaziçi University.

Reimer PJ, Baillie MGL, Bard E, Bayliss A, Beck JW et al. (2009). IntCal09 and Marine09 radiocarbon age

calibration curves, 0–50,000 years cal BP. Radiocarbon 51 (4): 1111–50. doi: 10.1017/S0033822200034202

Reynolds RL, Tuttle ML, Rice CA, Fishman NS, Karachewsk JA et al. (1994). Magnetization and geochemistry of greigite-bearing Cretaceous strata, north slope basin Alaska. American Journal of Science 294: 485–528. doi: 10.2475/ajs.294.4.485

Roberts AP, Turner GM (1993). Diagenetic formation of ferromagnetic iron sulphides minerals in rapidly deposited marine sediments, South Island, New Zealand. Earth and Planetary Science Letters 115: 257–273. doi: 10.1016/0012-821X(93)90226-Y

Roberts AP, Chang L, Rowan CJ, Horng VS, Florindo F (2011). Magnetic properties of sedimentary greigite (Fe_3S_4): an update. Reviews of Geophysics 49: 1002. doi: 10.1029/2010RG000336

Roberts AP (2015). Magnetic mineral diagenesis. Earth Science Review (151): 1-47. doi: 10.1016/j.earscirev.2015.09.010.

Ron H, Nowaczyk NR, Frank U, Schwab MJ, Naumann R et al. (2007). Greigite detected as dominating remanence carrier in late Pleistocene sediments, Lisan Formation, from Lake Kinneret (Sea of Galilee). Israel, Geophysical Journal of International 170: 117–131. doi: 10.1111/j.1365-246X.2007.03425.x

Saarinen, T (1998). High-resolution palaeosecular variation in northern Europe during the last 3200 years. Physics of the Earth and Planetary Interiors 106: 299–309. doi: 10.1016/S0031-9201(97)00113-1

Sagnotti L,Speranza F, Winkler A, Mattei, M, Funiciello R (1998). Magnetic fabric of clay sediments from the external northern Apennines (Italy). Physics of the Earth and Planetary Interiors 105: 73-93. doi: 10.1016/S0031-9201(97)00071-X

Sagnotti L, Macri P, Camerlenghi A, Rebesco M (2001). Environmental magnetism of Antarctic Late Pleistocene sediments and inter hemispheric correlation of climatic events. Earth and Planetary Science Letters 191: 65–80. doi: 10.1016/S0012-821X(01)00438-1

Sanver M, Ponat E (1981). İkiztepe I Kazısından elde edilen Arkeomanyetik Sonuçlar, TÜBİTAK Arkeometri Ünitesi Bilimsel Toplantı Bildirileri II. Boğaiçi Üniv. Yayınları.

Sarıbudak M, Tarling DH (1993). Archaeomagnetic Studies of the Urartian Civilization, Eastern Turkey. Antiquity 67: 620- 628. doi: 10.1017/S0003598X00045841

Sayın N, Orbay N (2003). Orta Anadolu Arkeomağnetik Örnekleri İle Yermagnetik Alanının Seküler Değişiminin İncelenmesi, İstanbul Üniv. Müh. Fak. Yerbilimleri Dergisi 16 (1): 33-43.

Shaar R, Hassul E, Raphael K, Ebert Y, Segal Y et al. (2018). The First Catalog of Archaeomagnetic Directions From Israel With 4,000 Years of Geomagnetic Secular Variations. Frontiers in Earth Science 6: 164 doi: 10.3389/feart.2018.00164

Snowball IF, Thompson R (1990). A stable chemical remanence in Holocene sediments, Journal of Geophysical Research 95: 4471–4479. doi: 10.1029/JB095iB04p04471.

Snowball IF (1991). Magnetic hysteresis properties of greigite (Fe3S4) and a new occurrence in Holocene sediments from Swedish Lappland. Physics of the Earth and Planetary Interiors 68: 32–40. doi: 10.1016/0031-9201(91)90004-2

Snowball I, Zillén L, Ojala A, Saarinen T, Sandgren P (2007). FENNOSTACK and FENNORPIS: Varve dated Holocene palaeomagnetic secular variation and relative paleointensity stacks for Fennoscandia. Earth and Planetary Science Letters 255: 106– 116. doi: 10.1016/j.epsl.2006.12.009

Snowball I, Sandgren P (2002). Geomagnetic field variations in northern Sweden during the Holocene quantified from varved lake sediments and their implications for cosmogenic nuclide production rates. Holocene 12: 517–530. doi: 10.1191/0959683602hl562rp

Tauxe L (1993). Sedimentary records of relative paleointensity of the geomagnetic field: theory and practice. Reviews of Geophysics 31: 319–354. doi: 10.1029/93RG01771

Thompson R, Turner GM, Stiller M and Kaufman A (1985). Near East palaeomagnetic secular variation recorded in sediments from the Sea of Galilee (Lake Kinneret). Quaternary Research 23: 175-188. doi: 10.1016/0033-5894(85)90027-4

Thompson R, Turner GM (1979). British geomagnetic master curves 10,000-0 yr B.P. for dating European, Geophysical Research Letters 6-4: 249–252.

Thomson J, Croudace IW, Rothwell RG (2006). A geochemical application of the ITRAX scanner to a sediment core containing eastern Mediterranean sapropel units. In: Rothwell, R.G. (Ed.), New Techniques in Sediment Core Analysis. Geological Society, London, Special Publications 267. doi: 10.1144/GSL.SP.2006.267.01.05

Valet JP (2003). Time variations in geomagnetic intensity. Reviews of Geophysics 41: 1004. doi: 10.1029/2001RG000104

Vigliotti L (2006). Secular variation record of the Earth's magnetic field in Italy during the Holocene: Constraints for the construction of a master curve. Geophysical Journal of International 165: 414–429. doi: 10.1111/j.1365-246X.2005.02785.x

Vigliotti L, Channell JET, Stockhecke M (2014). Palaeomagnetism of Lake Van sediments: chronology and palaeoenvironment since 350 ka. Quaternary Science Reviews 104: 1829. doi: 10.1016/j.quascirev.2014.09.028

Zijderveld JDA (1967). AC demagnetization of rocks: analysis of results, in Methods in Palaeomagnetism. In: Runcorn S.K., Creer K.M., Collinson D.W (editors) Elsevier, pp. 254–286